

THE GALAXY-GALAXY LENSING CONTRIBUTION TO THE COSMIC SHEAR TWO POINT FUNCTION

SARAH BRIDLE AND FILIPE B. ABDALLA

Department of Physics and Astronomy, University College London, Gower Street, London, WC1E 6BT, UK

Draft version August 16, 2018

ABSTRACT

We note that galaxy-galaxy lensing by non-spherical galaxy halos produces a net anti-correlation between the shear of background galaxies and the ellipticity of foreground galaxies. This anti-correlation would contaminate the tomographic cosmological weak lensing two point function if the effect were not taken into account. We compare the size of the galaxy-galaxy lensing contribution to the change in the cosmic shear two-point cross-correlation function due to a change in the dark energy equation of state w of 1%. We find them comparable on scales $\lesssim 5'$ for NFW galaxy profiles, and out to much larger scales for SIE profiles. However the galaxy-galaxy lensing signal has a characteristic spatial and redshift pattern which should allow it to be removed.

Subject headings: galaxies: halos — cosmology: dark matter — cosmology: cosmological parameters — cosmology: observations — cosmology: large-scale structure of universe

1. INTRODUCTION

Cosmic shear shows great promise for testing the cosmological model and measuring cosmological parameters. It measures the gravitational bending (lensing) of light by all the intervening mass in the Universe. In cosmic shear, distant (background) galaxies provide a convenient screen of objects with potentially simple statistical properties, from which the light bending can be inferred. The distortion depends on the lens geometry and thus on the curvature and expansion history of the Universe; it also depends on the distribution of matter, which itself depends on most aspects of the cosmological model.

Cosmic shear was first detected in 2000 (Wittman et al. 2000; Bacon et al. 2000; Van Waerbeke et al. 2000; Kaiser et al. 2000) and has been used to constrain cosmological parameters in subsequent surveys (recently Hoekstra et al. 2005). Cosmic shear has the potential to become the most powerful probe of cosmology because it observes a non-Gaussian three dimensional field in the local Universe, where the mysterious dark energy dominates. However a number of details inevitably remain to be investigated further whilst planning for future experiments.

The simplest statistic is the two point angular correlation function (or integrals of this quantity such as the power spectrum or aperture mass, Schneider 1996). If the background galaxies can be separated into populations at different redshifts the power of this statistic is greatly increased by cross-correlating galaxies in different redshift bins (Hu 1999). This technique will dominate for future surveys which aim to measure the equation of state of the dark energy, or determine a new gravitational theory.

Cosmic shear is particularly simple if distant background galaxies can be assumed to have random orientations. The distortion by gravitational lensing can then be extracted statistically, for example by averaging over galaxy orientations in a given patch of sky. Unfortunately it is unlikely to be straightforward since when galaxies form they tend to align pointing towards dark matter concentrations due to tidal interactions. This leads to two complicating effects: (i) neighbouring galaxies at a given redshift are intrinsically aligned (Hoyle 1949; Peebles 1969;

Heavens & Peacock 1988; Crittenden et al. 2001) and (ii) a pair of galaxies at two different redshifts have correlated observed ellipticities because a dark matter concentration close to the nearer object may tidally align the nearer object *and* simultaneously gravitationally lens the more distant object (Hirata & Seljak 2004).

These intrinsic alignment effects are complicated because they require an understanding of tidal alignments of galaxies, however they do have a distinctive signature and can therefore be removed without requiring a detailed understanding of galaxy formation (King & Schneider 2002, 2003; Heymans & Heavens 2003; King 2005).

In this paper we present another complicating effect which is much simpler than the intrinsic alignment effects: cross-correlation of a pair of galaxies at different redshifts produces a contribution to the usual cosmic shear two-point statistic even if there are no tidal effects. This is because the nearer galaxy will gravitationally lens the more distant galaxy (galaxy-galaxy lensing). This effect produces a net anti-correlation in the realistic case when the nearer galaxy (i) is not circularly symmetric and (ii) has a correlation between the asymmetry of the light and the mass. In this paper we present this new factor and quantify its effect for elliptical dark matter halos for which mass and light have the same ellipticity and orientation.

First we review ellipticity and shear correlation function notation. We then illustrate the galaxy-galaxy lensing contribution to the ellipticity correlation function and calculate the effect due to a population of galaxy lenses at a fixed redshift. We investigate how this effect depends on the source and lens redshift. Finally we compare this to the size of the tomographic cosmic shear cross-correlation signal.

2. THE ELLIPTICITY CORRELATION FUNCTION

The two-point correlation function of the shear field $\gamma(\mathbf{x})$ at positions separated by an angle θ on the sky is given by $\xi_\gamma = \langle \gamma\gamma^* \rangle$, averaging over all pairs of angular separation θ (We use complex notation for shears $\gamma = \gamma_1 + i\gamma_2$ and similarly for ellipticities.) For a concise introduction to cosmic shear see Refregier (2003); see also Mellier (1999) and Bartelmann & Schneider (2001).

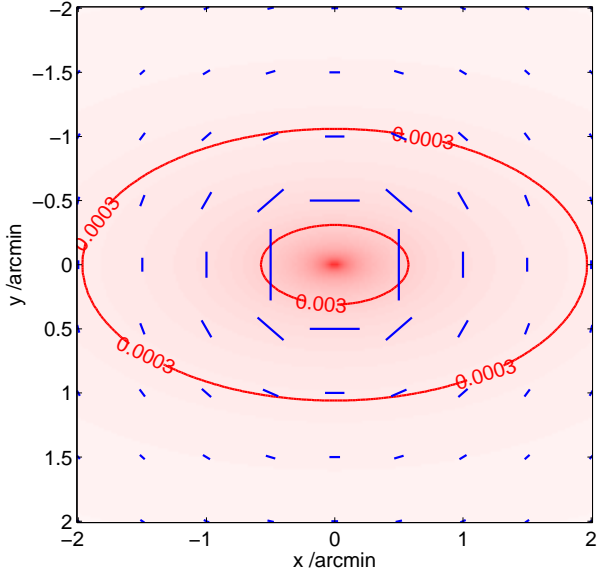


FIG. 1.— Shading and contours show the convergence for an elliptical NFW mass distribution ($e = 0.3$, $M_{200} = 1.2 \times 10^{12} M_{\odot}/h$) at a redshift of 0.3 with sources at redshift 0.8. Lines show the resulting shear map. Note that sticks on the x axis are larger than sticks on the y axis for same distance from the lens center.

Cosmic shear aims to measure this correlation function by measuring observed ellipticities of distant galaxies e^o and taking into account how intrinsic (pre-shear) ellipticities e^i are modified by shear. For small shears this reduces to $e^o = e^i + \gamma$; we define $e \equiv (a - b)/(a + b)$ throughout. An estimate of the shear two point correlation function is obtained from the observed ellipticity correlation function $\xi_e = \langle e_s^o e_d^{o*} \rangle$ where e_s^o is the observed ellipticity of a distant galaxy s and e_d^o is that of a nearer galaxy d. Therefore we can expand the correlation functions to find $\xi_e = \xi_{\gamma} + \xi_{\gamma e}$, where the shear-ellipticity correlation is given by $\xi_{\gamma e} = \langle \gamma_s e_d^{i*} \rangle$ if we ignore intrinsic alignments ($\langle e_s^i e_d^{i*} \rangle = 0$) and use $\langle e_s^i \gamma_d \rangle = 0$.

Heymans et al. (2006) calculated the shear-ellipticity correlation function numerically using n-body simulations. The aim of that work was to quantify the intrinsic alignment - shear correlation presented by Hirata & Seljak (2004). Their results should in fact contain a mixture of the intrinsic alignment - shear correlation and the galaxy-galaxy lensing signal we present here. However, they do not discuss the distinction between the two effects, or specifically state that the galaxy-galaxy lensing contribution might be significant. Here we present simple analytical and numerically integrated results to quantify only the galaxy-galaxy lensing contribution.

We assume a concordance Λ CDM cosmology throughout, with parameters taken from Spergel et al. (2006): Hubble constant $H_0 = 73 \text{ km s}^{-1} \text{ Mpc}^{-1}$, $\Omega_m = 0.238$, $\Omega_{DE} = 1 - \Omega_m$, $\Omega_b = 0.047$, $\sigma_8 = 0.74$, dark energy equation of state $w = -1$ except where otherwise stated. We assume a flat universe with a scale invariant primordial power spectrum.

3. THE GALAXY-GALAXY LENSING CONTRIBUTION

In this Section we calculate the galaxy-galaxy lensing contribution to ξ_e , given by $\xi_{\gamma e}$, as discussed above. To estimate this quantity we first calculate the signal for a single elliptical lens averaged over background galaxies at a

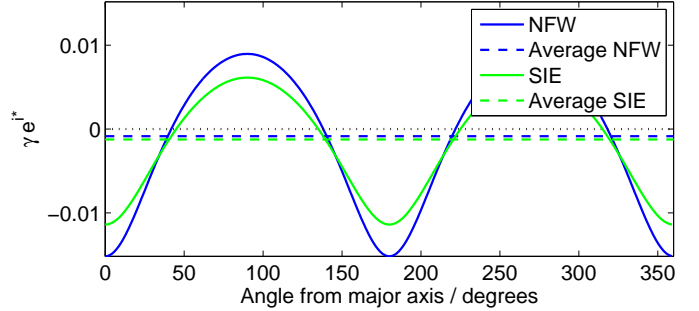


FIG. 2.— *Solid lines*: the shear-ellipticity correlation (γe^{i*}) at an angular separation of $0.1'$ for a single lens. *Larger amplitude solid line*: For the elliptical NFW shown in Fig 1. *Smaller amplitude solid line*: For an SIE with the same M_{200} . *Upper dashed line*: Outer solid line averaged over angle. *Lower dashed line*: Inner solid line averaged over angle. In both cases the variation mostly cancels leaving a negative shear-ellipticity correlation. Note that averaging over many background galaxies with many position angles is equivalent to integrating under the sine-like curve and the effect persists. In this case the shear-ellipticity correlation is simply a rescaling of the shear by a factor of $e = 0.3$.

fixed angular distance, and then average over a population of lenses. We assume that the lens light has the same ellipticity and orientation as the lens mass.

By default we consider an NFW (Navarro et al. 1997) mass profile, calculating the projected mass from the equations given in Wright & Brainerd (2000) and Bartelmann (1996). We use M_{200} , the mass enclosed within the radius at which the density is 200 times the mean density of the Universe, for consistency with simulations. We derive the concentration parameter, c , as a function of M_{200} using Eq. 12 of Seljak (2000) with $\beta = -0.15$, as appropriate for an NFW model.

We calculate the shear for an elliptical mass distribution using the equations in Keeton (2001) and Schramm (1990). Note that this is not the same as calculations using elliptical potentials, which give dumbbell shaped mass distributions (e.g., Kassiola & Kovner 1993). The projected mass distribution is squashed and stretched to have elliptical isodensity contours a factor f smaller (larger) along the minor (major) axes, as compared to the corresponding spherical mass distribution.

The shear map for an elliptical NFW lens of ellipticity $e = 0.3$ aligned along the x axis is shown in Fig. 1. The shading and contours show the convergence map (projected mass density in units of the critical lens density). The overlaid shear sticks show two particularly interesting features: (i) the shear on the major axis of the lens is larger than that on the minor axis, for a given angular separation from the lens center; (ii) the shear 45 degrees around from the major axis is approximately tangential to the center of the lens. These two features do depend on the details of the mass profile, but are general for relevant radii for an elliptical NFW profile, and also for a singular isothermal ellipsoid (SIE) (for which the shear is always exactly tangential and its amplitude follows the mass, see Kassiola & Kovner 1993; Kormann et al. 1994).

These two characteristics point towards our main result: that there is a net anti-correlation between lens ellipticity and the resulting shear of background galaxies. This arises because (i) the shears on the major and minor axes cancel out, but only partially, leaving a shear which is perpendicular to the major axis of the lens; (ii) the shear sticks

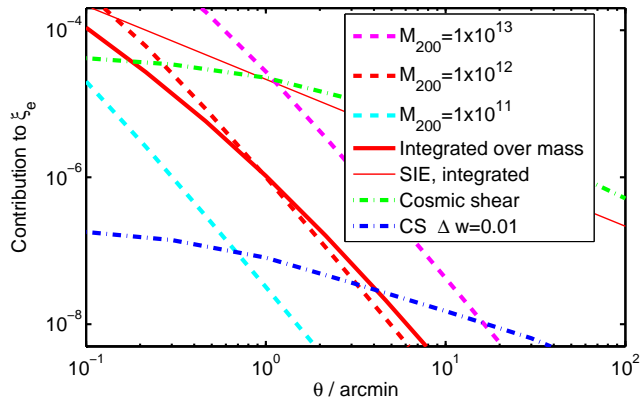


FIG. 3.— *Dashed lines*: The galaxy-galaxy lensing contribution to the ellipticity correlation function for lenses of varying mass (from lowest to highest: $1 \times 10^{11} M_{\odot}/h$, $1 \times 10^{12} M_{\odot}/h$ and $1 \times 10^{13} M_{\odot}/h$; $|e| = 0.2$, $z_d = 0.3$, $z_s = 0.8$). (Absolute values are shown; The correlation is negative at all scales and masses.) *Thick solid line*: Averaged over an $R < 24$ population with rms ellipticity of each component 0.16 ($z_d = 0.3$, $z_s = 0.8$). *Thin solid line*: As for thick solid line but for a SIE profiles instead of elliptical NFWs. *Upper dash-dot line*: The cosmic shear two point correlation function between redshift 0.3 and 0.8. *Lower dash-dot line*: The difference between cosmic shear correlation functions with dark energy equation of state values $w = -1$ and $w = -0.99$.

in-between the major and minor axes do not remove this anti-correlation (for example this could have happened had the shear sticks been aligned along iso-density contours).

This is quantified in detail in Fig. 2, which shows the shear-ellipticity correlation for a lens at $z = 0.3$ with a background source at $z = 0.8$, but as a function of θ around the lens center (consider moving around a concentric circular annulus in Fig. 1). The integral under this curve shows the net effect of averaging over galaxies.

The shape of the curve is non-trivial, but on average is below zero, as shown by the dashed lines. The larger amplitude oscillation is for the elliptical NFW shown in Fig. 1, and the smaller oscillation is for an SIE with the same M_{200} . They both show the same qualitative effect at the radius used for the figure (0.1 arcmin). At larger radii, for the SIE, the average shear-ellipticity correlation remains a similar fraction of the maximum due to the scale independence of the SIE. For the NFW profile, the average becomes a smaller fraction of the maximum due to the steepening of the NFW profile with radius.

The middle dashed line in Fig. 3 shows this average quantity as a function of angular separation for a single lens of mass $10^{12} M_{\odot}/h$ and ellipticity 0.2. The other dashed lines show how the effect depends on lens mass.

So far we have shown that for a single foreground lens there is an anti-correlation between shear and lens ellipticity. We now compare the cosmic shear tomographic cross correlation (ξ_{γ}) with the average of ξ_{γ_e} over all foreground lenses. Qualitatively: the shear-ellipticity correlation for a single lens is a scalar quantity, and therefore is independent of the angle of the coordinate system. As a result, on averaging over many isolated lenses at different angles to each other, the anti-correlation will be preserved: we average many negative numbers ($\gamma e^{i\phi}$ for each lens) together and still obtain a negative number. This assumes that the foreground lenses are isolated from each other, and that there is no additional lensing from structures the foreground lenses are aligned with (i.e. ignores the intrinsic

alignment – shear correlation).

We now quantify the effect of averaging over many isolated lenses at a given redshift. First we assume all lenses have the same mass and consider just the variety of ellipticities. We average over a population of lens ellipticities, drawing each ellipticity component from a Gaussian of width 0.16, and calculating the absolute ellipticity. We find that the shear-ellipticity correlation scales roughly as the square of the lens ellipticity. This implies that the mean shear scales with lens ellipticity. The shear-ellipticity correlation function, after averaging over this population, is roughly equal to that for a single lens of ellipticity 0.23. As expected from the squared dependence, this is slightly higher than the mean absolute ellipticity of the lenses (0.20).

We also average over the lens population mass distribution expected for a survey with shear measurements complete to an apparent magnitude limit of 24 in the SDSS r filter. We obtain number densities from Sheth & Tormen (1999) calculated at the lens redshift, down to a limiting mass M_{lim} which corresponds to the magnitude limit. This limiting mass was determined by (i) calculating from the mass function the number of objects per unit volume integrated down to the limiting mass (ii) comparing this with number density of observed galaxies derived from COMBO-17 luminosity functions (Wolf et al. 2003), using the numbers in Table 1 of Blake & Bridle (2005). We find $M_{\text{lim}} = 3 \times 10^{10} M_{\odot}/h$, which gives a mean mass of $4 \times 10^{11} M_{\odot}/h$.

We investigated the effect of averaging over mass by considering the contribution to ξ_e for a fixed lens ellipticity. At 4 arcmin the ξ_e contribution averaged over mass is equal to that for a single lens of mass $1.2 \times 10^{12} M_{\odot}/h$. This is bigger than the mean mass of the objects because the dependence of the shear-ellipticity correlation is roughly $M^{1.5}$ at this angular scale.

The thick solid line in Fig. 3 shows the contribution to the ellipticity correlation function after averaging over mass and ellipticity. It is slightly more shallow than the lines at constant mass since larger masses dominate at larger angular separations due to their smaller concentration parameters. This is slightly amplified by the fact that larger ellipticities contribute more at larger radii, and larger ellipticities have a larger shear-ellipticity correlation.

To estimate the dependence on lens profile we repeat the above calculations using a population of SIE lenses, with velocity dispersions calculated analytically from M_{200} . The resulting contribution is shown by the thin solid line in Fig. 3, and is much higher than the NFW result, likely mainly because of the shallower density profile at large radii ($\propto r^{-2}$ instead of $\propto r^{-3}$).

All of the above calculations assume a lens redshift of $z_d = 0.3$ and a background redshift of $z_s = 0.8$. The solid lines in Fig. 4 show how the signal at 4 arcmin depends on lens and source redshift. In general the signal is larger at lower lens redshifts and decreases rapidly to zero as the lens approaches the source. We expect the signal to be smaller as the lens approaches the source because of the geometry of gravitational lensing. The fact that it drops so quickly, and in fact for $z_s = 1.2$ rises slightly first, is because at higher redshifts a magnitude limited survey contains more massive objects, that are more effective at

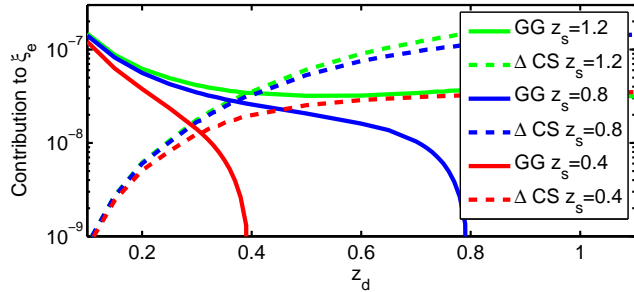


FIG. 4.— *Solid lines*: Dependence of the galaxy-galaxy lensing shear-ellipticity correlation at 4 arcmin on lens redshift for source redshifts 0.4, 0.8 and 1.2 (lower, middle and upper lines respectively). *Dashed lines*: Cosmic shear cross-correlation between a sample at a redshift z_l and samples at redshifts $z_s = 0.4, 0.8$ and 1.2 (lower, middle and upper lines respectively); for a change in w of 0.01 (the result for $w = -0.99$ is subtracted from the result for $w = -1$).

lensing. At low redshift, galaxies have a larger angular size so for a given angular separation we start to probe into the center of the NFW profile where the profile slope is more constant with radius. However, on averaging over redshift the lower redshift contribution would become smaller since there will be fewer objects in the light cone. Also there is little cosmic shear signal at low redshift so these galaxies could be ignored.

Finally we investigated the effect of survey depth, and find that for a given angular scale, fixing $z_d = 0.3$ and $z_s = 0.8$, the signal was around a factor 2.5 larger if $r < 22$, and a factor approximately 4 smaller if $r < 27$, depending on the extrapolation of the luminosity function. This is to be expected because deeper surveys contain many less massive objects.

4. DISCUSSION

In Figs. 3 and 4 we compare the galaxy-galaxy lensing contribution to the ellipticity correlation function with that from cosmic shear cross-correlation tomography. We calculate the non-linear matter power spectrum as a function of redshift using CAMB (Lewis et al. 2000) with the HaloFit (Smith et al. 2003) option. This is converted into the cosmic shear cross power spectrum using equations from Hu (1999). We assume delta function redshift distributions corresponding to the galaxy-galaxy lens and source redshifts.

The cosmic shear correlation function is flatter than the galaxy-galaxy lensing contribution. Above $\sim 0.2'$ the galaxy-galaxy lensing contribution is smaller than the cosmic shear signal for NFW lenses. However it must be much smaller than the cosmic shear signal if it is not to interfere with cosmological parameter analyses.

To illustrate this we also show the change in cosmic shear signal for a small change ($\Delta w = 0.01$) in the equation of state of dark energy, w , leaving the other cosmological parameters (including σ_8) fixed. The galaxy-galaxy lensing contribution is not negligible below 4 arcmin for NFW galaxy profiles. We find that this scale will strongly depend on the lens profile since it is greater than 30 arcmin for SIE profiles.

We assumed that the lens ellipticity is the same size and orientation as the mass ellipticity. This is consistent with measurement attempts (Hoekstra et al. 2004; Mandelbaum et al. 2006), but the signal to noise is low. If the mass ellipticity were a factor f smaller than the light then this would simply scale the galaxy-galaxy lensing contribution by f . If there is a misalignment then the effective f on stacking would be a first approximation to the change. Heymans et al. (2006) consider a more sophisticated alignment model which can reduce the signal by a factor of roughly three.

It would be interesting to see whether the contribution is increased or reduced on considering clustering of the lens galaxies. Further, it is not clear whether deviations from ellipsoidal symmetry of the lens (such as substructures) would average out.

A rough comparison of Fig. 3 with Heymans et al. (2006) (Table 2) indicates that at 1 arcminute the galaxy-galaxy NFW lensing contribution is a significant fraction of the total shear-intrinsic alignment correlation, whereas at 10 arcmin the shear-intrinsic alignment correlation is dominated by tidal alignments. Note that this comparison is only approximate since Heymans et al. (2006) integrate over lens redshift.

Fortunately it may be relatively easy to remove the galaxy-galaxy lensing contribution using the characteristic tangential nature of galaxy-galaxy lensing. For example the ellipticity two-point function could be measured as a function of two dimensional separation (θ_1, θ_2) , where the position angle α is measured from the major axis of the foreground lens. (This “stack and rotate” method was advocated by Natarajan & Refregier 2000, to measure ellipticity of galaxy dark matter halos.) The galaxy ellipticity and profile could then be fitted simultaneously with extracting the cosmic shear two point function. Alternatively one could use the method of King (2005), which uses the redshift signature of the effect. Also Heymans et al. (2006) suggest removing the most luminous galaxies in the lower redshift slice.

This effect should also ultimately be taken into account for higher order statistics of cosmic shear, since they probe smaller scales than the two-point statistic (see ?, for a calculation for the three point function). Furthermore the galaxy-galaxy flexion signal could be a bigger contaminant of cosmic flexion because the latter is more sensitive than cosmic shear at small angular scales.

We thank Keith Biner, Masahiro Takada, Peter Schneider, Virginia Corless, Eduardo Cypriano, David Sutton, Phil Marshall, Richard Massey, Fergus Simpson, Adi Nusser and Lindsay King for helpful discussions. SLB acknowledges support from a Royal Society University Research Fellowship.

REFERENCES

- Bacon, D., Refregier, A., & Ellis, R. 2000, MNRAS, 318, 625
 Bartelmann, M. 1996, A&A, 313, 697
 Bartelmann, M. & Schneider, P. 2001, Phys. Rep., 340, 291
 Blake, M. & Bridle, P. 2005, MNRAS, 363, 1329
 Crittenden, R., Natarajan, P., Pen, U.-L., & Theuns, T. 2001, ApJ, 559, 552

- Heavens, A., & Peacock, J. 1988, MNRAS, 232, 339
- Heymans, C. & Heavens, A. 2003, MNRAS, 339, 711
- Heymans, C., White, M., Heavens, A., Vale, C. & Van Waerbeke, L. 2006, MNRAS, 339, 711
- Hirata, C. M. & Seljak, U. 2004, Phys. Rev. D, 70, 063526
- Hoekstra, H. et al. astro-ph/0511089
- Hoekstra, H., Yee, H. K. C., & Gladders, M. D. 2004, ApJ, 606, 67
- Hoyle, F. 1949, Problems of Cosmical Aerodynamics, p. 195
- Ho, S. & White, M. 2003, ApJ, 607, 40
- Hu, W. 1999, ApJ, 522, L21
- Kaiser, N., Wilson, G., & Luppino, G. A. astro-ph/0003338
- Kassiola, A. & Kovner, I. 1993, ApJ, 417, 450
- Keeton, C. R. astro-ph/0102341
- King, L. & Schneider, P. 2002, A&A, 396, 411
- King, L. J. 2005, A&A, 441, 47
- King, L. J. & Schneider, P. 2003, A&A, 398, 23
- Kormann, R., Schneider, P., & Bartelmann, M. 1994, A&A, 284, 285
- Lewis, A., Challinor, A., & Lasenby, A. 2000, ApJ, 538, 473
- Mandelbaum, R., Hirata, C. M., Broderick, T., Seljak, U., & Brinkmann, J. 2006, MNRAS, 370, 1008
- Mellier, Y. 1999, ARA&A, 37, 127
- Natarajan, P. & Refregier, A. 2000, ApJ, 538, L113
- Navarro, J., Frenk, C., & White, S. 1997, ApJ, 490, 493
- Peebles, J. 1969, ApJ, 155, 393
- Refregier, A. 2003, ARA&A, 41, 645
- Schneider, P. 1996, MNRAS, 283, 837
- Schramm, T. 1990, A&A, 231, 19
- Seljak, U. 2000, MNRAS, 318, 203
- Sheth, R. K. & Tormen, G. 1999, MNRAS, 308, 119
- Smith, R. et al. 2003, MNRAS, 341, 1311
- Spergel, D. N. et al. astro-ph/0603449
- Van Waerbeke, L. et al. 2000, A&A, 358, 30
- Wittman, D. M., Tyson, J. A., Kirkman, D., Dell'Antonio, I., & Bernstein, G. 2000, Nature, 405, 143
- Wolf, C. and Meisenheimer, K. and Rix, H.-W. and Borch, A. and Dye, S. and Kleinheinrich, M. 2003, A&A, 401, 73
- Wright, C. O. & Brainerd, T. G. 2000, ApJ, 534, 34